

This article was downloaded by: [Siaulių University Library]

On: 17 February 2013, At: 07:09

Publisher: Taylor & Francis

Informa Ltd Registered in England and Wales Registered Number: 1072954

Registered office: Mortimer House, 37-41 Mortimer Street, London W1T 3JH, UK



Advanced Composite Materials

Publication details, including instructions for authors and subscription information:

<http://www.tandfonline.com/loi/tacm20>

Impact perforation of orthotropic and quasi-isotropic CFRP laminates by a steel ball projectile

Hideaki Kasano

Version of record first published: 02 Apr 2012.

To cite this article: Hideaki Kasano (2001): Impact perforation of orthotropic and quasi-isotropic CFRP laminates by a steel ball projectile , Advanced Composite Materials, 10:4, 309-318

To link to this article: <http://dx.doi.org/10.1163/156855101753415337>

PLEASE SCROLL DOWN FOR ARTICLE

Full terms and conditions of use: <http://www.tandfonline.com/page/terms-and-conditions>

This article may be used for research, teaching, and private study purposes. Any substantial or systematic reproduction, redistribution, reselling, loan, sub-licensing, systematic supply, or distribution in any form to anyone is expressly forbidden.

The publisher does not give any warranty express or implied or make any representation that the contents will be complete or accurate or up to date. The accuracy of any instructions, formulae, and drug doses should be independently verified with primary sources. The publisher shall not be liable for any loss, actions, claims, proceedings, demand, or costs or

damages whatsoever or howsoever caused arising directly or indirectly in connection with or arising out of the use of this material.

Impact perforation of orthotropic and quasi-isotropic CFRP laminates by a steel ball projectile

HIDEAKI KASANO*

Department of Mechanical Systems Engineering, Takushoku University, 815-1 Tate-machi, Hachioji City, Tokyo 193-0985, Japan

Abstract—This paper considers the perforation characteristics of orthotropic and quasi-isotropic carbon fiber composite laminates struck by a steel ball projectile, both analytically and experimentally. Two analytical models, which are developed on the basis of the conservation laws of momentum and/or energy, are introduced. High velocity impact tests by a steel ball projectile are also conducted on the CFRP target plates. By combining these models with the test results, simple semi-empirical expressions for estimating/predicting the perforation characteristics of these CFRP laminates are presented. The ballistic limit velocities estimated from the semi-empirical expression agree well with those obtained by applying the statistical approach to the test data. Comparison of the residual velocities also shows a fairly good agreement between those predicted from the expression and obtained from the impact tests.

Keywords: Impact perforation; orthotropic and quasi-isotropic CFRP laminates; analytical modeling; steel ball projectile; perforation characteristics.

1. INTRODUCTION

Impact perforation of plates by projectiles covers a variety of protective structures in civil applications as well as in military ones. In the design of the protective structures, perforation characteristics are of critical importance and a most commonly used measure of the preventability of perforation is a ballistic limit velocity which is the greatest projectile velocity the structure can resist without perforation. Therefore, many investigations on the estimate of ballistic limit velocities have been made [1, 2]. On the other hand, a residual velocity of a projectile after perforating a target plate is equally important, and so just as much work has been done on the prediction of residual velocity. Most of these papers have been concerned exclusively with concrete and metallic plates. In recent years, however, attention is

*E-mail: hkasano@ms.takushoku-uac.jp

also being attracted to fiber composite laminates such as glass, carbon, and aramid fiber reinforced plastic composites, since they are expected to be used for structural applications threatened by high velocity impact [3–5]. Recent works on impact perforation of fiber composite laminates struck by foreign objects traveling at high speed have been reviewed by the present author [6].

The purpose of this work is to examine the perforation characteristics of carbon fiber composite laminates struck by a steel ball projectile, both analytically and experimentally. Two analytical models are introduced. The first model is based solely on the energy conservation law, while the second involves both the momentum and the energy conservation laws. High velocity impact tests by a steel ball projectile are also conducted on the orthotropic and the quasi-isotropic CFRP composite laminates. By combining these models with the test results, simple semi-empirical expressions for estimating/predicting the perforation characteristics are presented.

2. PERFORATION MECHANICS

2.1. General expressions for residual velocity and ballistic limit velocity

Consider a steel ball projectile impinging on a target plate and passing through it as shown in Fig. 1. A residual velocity V_R of the projectile after perforating the target plate is a function of many factors associated with the projectile, the target plate, and impact condition. Hence, in general, it may take the form of

$$V_R = F(a_1, a_2; V_i, \Psi), \quad (1)$$

where a_1 represents material properties of the projectile and target plate; a_2 , the initial geometry of the projectile and target plate; V_i , the impact velocity of the projectile; and Ψ is a measure of the obliquity $= (\phi, \theta)$. A ballistic limit velocity V_b is another perforation characteristic and it is the velocity beyond which a specified projectile perforates a specified target plate and below which it will not. Hence, it is defined mathematically as follows:

$$V_b = \max\{V_i : V_R = 0\} = \inf\{V_i : V_R > 0\}. \quad (2)$$

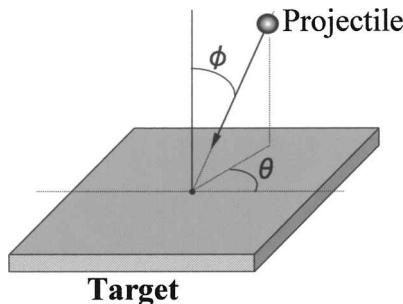


Figure 1. A steel ball projectile impinging on and passing through a target plate.

Thus, by putting $V_R = 0$ and $V_i = V_b$ in equation (1), we have

$$0 = F(a_1, a_2; V_b, \Psi),$$

and, from this equation, the ballistic limit velocity must have the following form:

$$V_b = G(a_1, a_2; \Psi). \quad (3)$$

The ballistic limit velocity given by equation (3) is one of the parameters affecting the residual velocity, so the expression (1) may also be rewritten in the form

$$V_R = \overline{F}(a_1, a_2, V_b; V_i, \Psi). \quad (4)$$

2.2. Governing equations

For simplicity, we consider only a normal impact ($\phi = 0$) of a steel ball projectile on a target plate. The projectile is assumed here to pass through the plate accompanied by plate-fragments, as illustrated in Fig. 2, in which V_i is the impact velocity of a projectile; V_R , the residual velocity of the projectile; v_R is the flying velocity of the plate-fragments; M , the mass of the projectile; and m is the total mass of the fragments ejected from the plate due to perforation. This perforation process is described by three fundamental conservation laws in the impact dynamics: conservation of mass, momentum, and energy. Since mass is assumed to be conserved in this system, the following two conservation laws provide the governing equations for the analysis:

$$MV_i = MV_R + mv_R + I, \quad (5)$$

$$\frac{1}{2}MV_i^2 = \frac{1}{2}MV_R^2 + \frac{1}{2}mv_R^2 + E_P, \quad (6)$$

where I is the impulse transmitted to the plate and $E_P = E_P(V_i)$ is the total energy lost during the perforation process.

2.3. Analytical modeling

Two analytical models are introduced to estimate the ballistic limit velocity and predict the residual velocity for CFRP target plates. Model A employs the conservation law of energy alone, in which the perforation energy E_P is assumed to be independent of the impact velocity exceeding the ballistic limit velocity and it

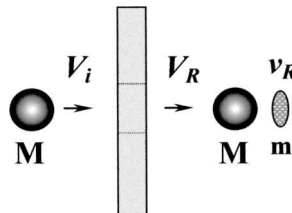


Figure 2. Perforation process accompanied by plate-fragments.

remains constant. Meanwhile, in Model B [7], the conservation laws of momentum and energy are used, where the perforation energy is separated into two parts, i.e. inelastic deformation energy E_{Pf} associated with a free impact of a projectile and a target plate, and the shear deformation energy E_{Ps} required for the removal of the fragments from the plate. The latter is also assumed to remain constant for the impact velocity greater than the ballistic limit velocity. These two models formally lead to the same expressions for estimating/predicting the ballistic limit velocity and the residual velocity as follows:

$$V_b = \sqrt{V_i^2 - V_R^2/\alpha^2}, \quad (7)$$

$$V_R = \alpha \sqrt{V_i^2 - V_b^2}, \quad (8)$$

where the mass coefficient α is given by

$$\alpha = \left(\frac{M}{M+m} \right)^{1/2}, \quad \alpha = \frac{M}{M+m}, \quad (9)$$

for Models A and B, respectively.

For a pair of V_i and V_R along with α obtained from an impact test, the corresponding V_b is calculated from equation (7). A mean value of these V_b 's thus obtained for some different pairs of V_i and V_R can be regarded as an estimated ballistic limit velocity. The ballistic limit velocity being determined, the residual velocity is predicted from equation (8) as a function of the impact velocity.

3. TARGET MATERIALS AND IMPACT TESTS

3.1. Target materials

CFRP composite laminates were chosen as the target materials. The panels are first fabricated by laying up unidirectional carbon fiber prepreg sheets, where three kinds of stacking sequence are employed, and then they are cut into square plates of 90 mm by 90 mm. The orthotropic plates have the stacking sequence of $[0/90/0]_{ns}$, in which $n = 2$ and 3 are adopted in the impact tests. The quasi-isotropic plates, on the other hand, are of $[0/+45/-45/90]_{ns}$ and $[-60/0/60]_{ns}$, where $n = 1, 2$, and 3 are used. These plates are denoted by A_n , B_n , and C_n , respectively. The plate-thickness ranges between 0.9 mm and 3.6 mm.

3.2. Impact testing machine

Figure 3 shows a gas-gun impact testing machine. A steel ball projectile of 5 mm in diameter and 0.51 g by weight is propelled by releasing high pressurized nitrogen gas in a chamber and it impinges on a target plate. The testing machine is capable of firing the projectile at a maximum velocity of around 330 m/s. The impact velocity V_i , which is the velocity of the projectile just before impact, is determined from the

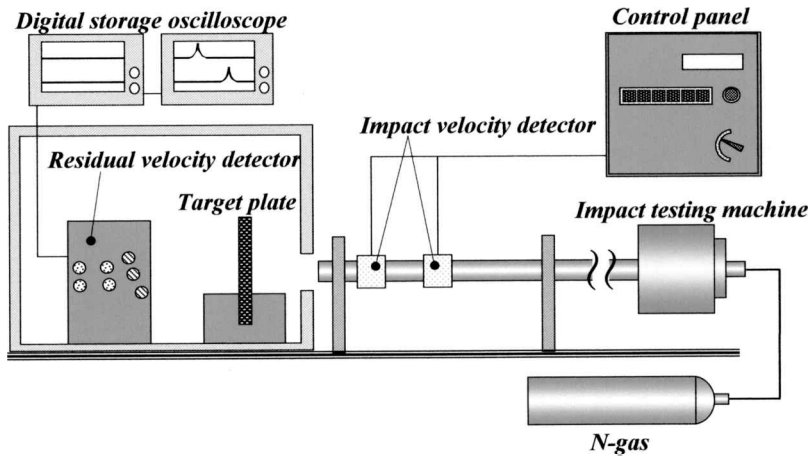


Figure 3. Schematic drawing of impact testing machine.

time of the projectile traveling between two specified points measured by a laser velocity detector located at the end of the barrel. The residual velocity V_R after perforating the target plate is also determined in a like manner by an infrared ray sensors located behind the plate.

3.3. Test procedure

The target plates are mounted in the fixture and struck normally by a steel ball projectile. The right and left edges are both clamped by the frames in the testing, while the upper and lower edges are free. The impact velocities vary between about 180–280 m/s for A_n plates, 120–320 m/s for B_n and C_n plates. For each test, an impact velocity V_i , the corresponding residual velocity V_R , and mass of the plate-fragments m are measured.

4. RESULTS AND DISCUSSIONS

Figure 4 shows the residual velocity as a function of impact velocity for the A_n , B_n , and C_n target plates, in which the open symbols represent the experimental results. The residual velocity increases parabolically near to the ballistic limit velocity and then linearly increases with an increasing impact velocity. The ballistic limit velocities shown in the figures are obtained by substituting a pair of residual and impact velocities together with a mass coefficient into equation (7) and then by averaging the values thus obtained for some pairs of V_i , V_R , and α . In this way, a ballistic limit velocity is estimated for each target plate. If the ballistic limit velocity is substituted into equation (8), the residual velocity is predicted for a given impact velocity. Solid lines represent the predictions from the semi-empirical expression for a residual velocity of a projectile when an impact velocity is given. Comparison of the predictions with the experimental results shows a fairly good agreement.

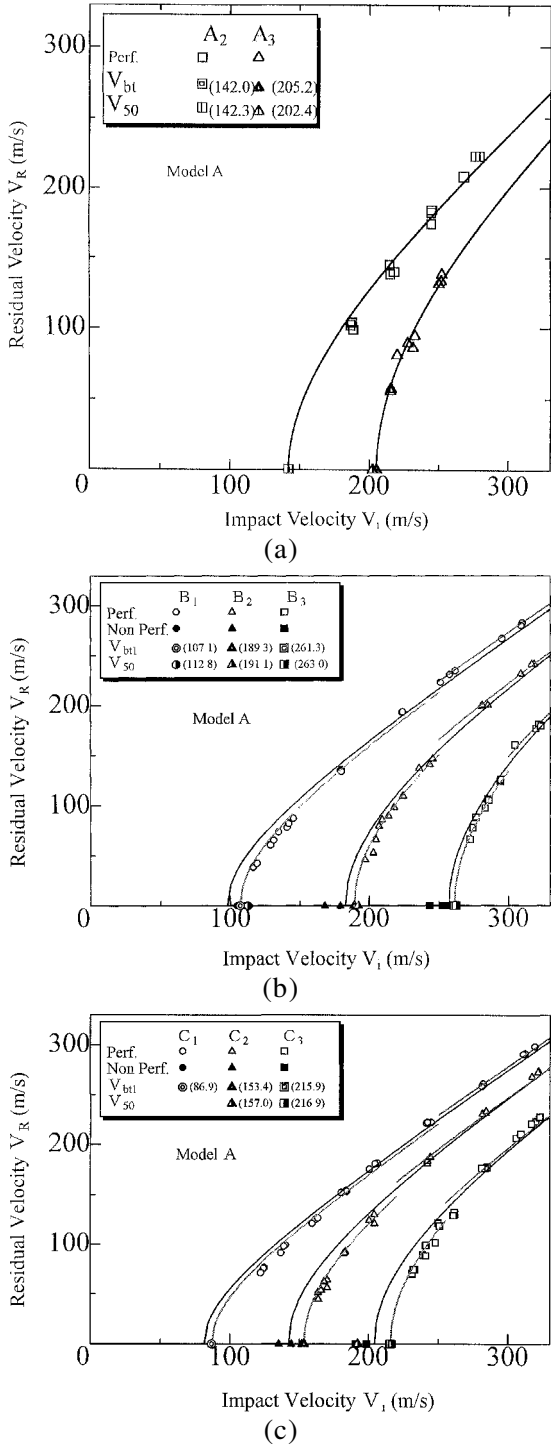
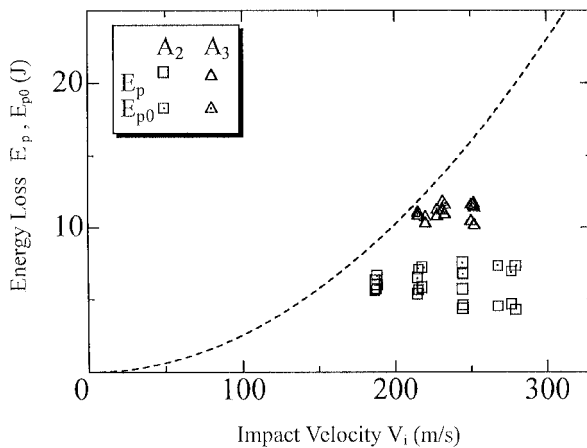
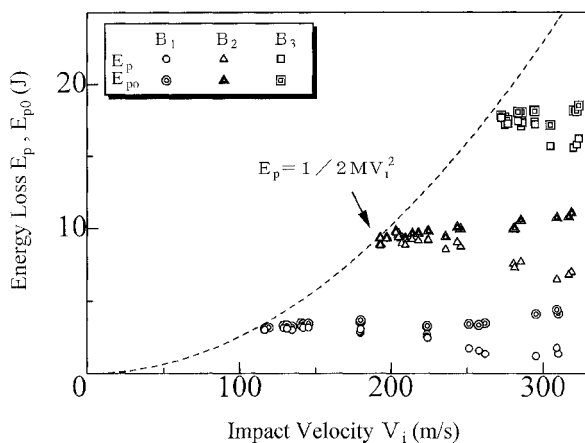


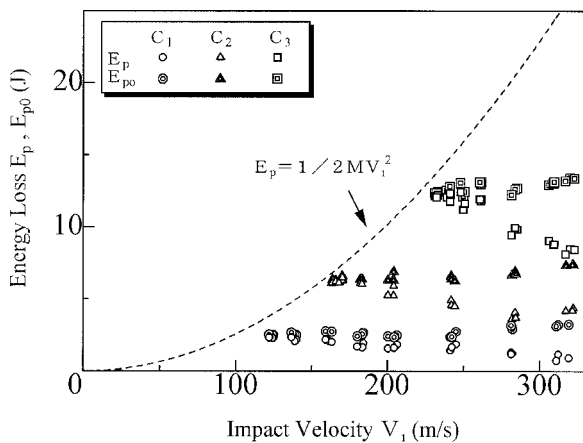
Figure 4. Residual velocity as a function of impact velocity. (a) A_n plate, (b) B_n plate, (c) C_n plate.



(a)



(b)



(c)

Figure 5. Energy loss as a function of impact velocity. (a) A_n plate, (b) B_n plate, (c) C_n plate.

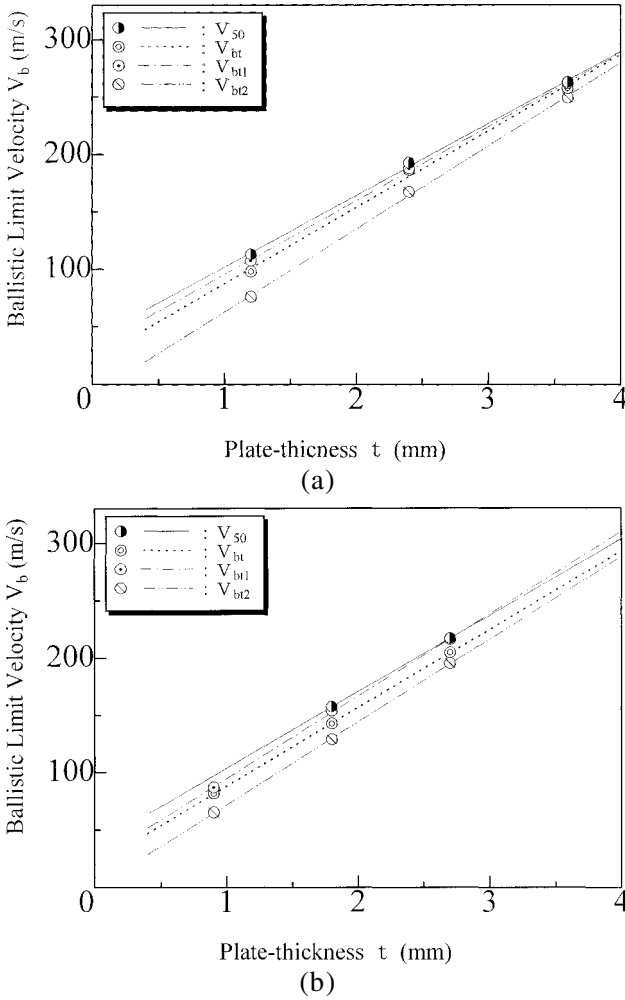


Figure 6. Four kinds of ballistic limit velocities as a function of plate-thickness. (a) B_n plate, (b) C_n plate.

Figure 5 shows the total perforation energy $E_P(V_i)$ lost during the perforation and the loss of the kinetic energy $E_{P0}(V_i)$ of the projectile as a function of impact velocity. Both energies remain almost constant for the impact velocity exceeding and close to the ballistic limit velocity. As the impact velocity increases, however, the total perforation energy tends to slightly decrease, while the loss of the kinetic energy increases. This is more remarkable for quasi-isotropic B_n and C_n plates than for the orthotropic A_n plate. For further increased impact velocity, both energies come to an almost constant value again. This fact requires the modification of the analytical modeling in which a constant total perforation energy is assumed for the impact velocity over the ballistic limit velocity. Therefore, the assumption is applied separately to the two impact velocity ranges close to and far away from the ballistic

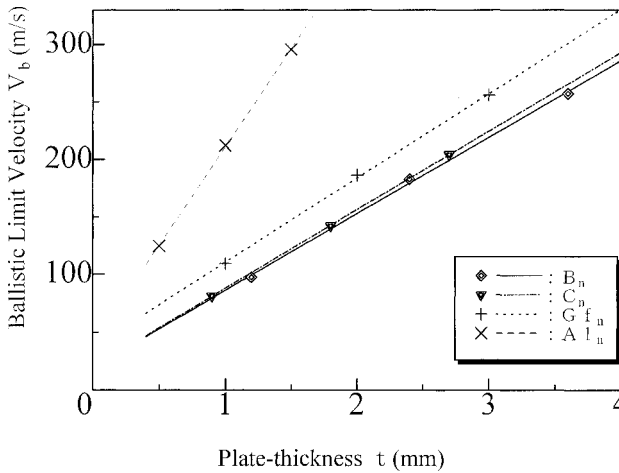


Figure 7. Comparison of ballistic limit velocities for B_n and C_n plates.

limit velocity. The ballistic limit velocities V_{bt1} shown in Figs 4b and 4c are those estimated from the modified analytical models for the impact velocity range close to the ballistic limit velocity. The ballistic limit velocity thus obtained is found to be in good agreement with V_{50} , i.e. that of a 50% probability of perforation that is estimated by applying the statistical approach to the test data.

Figure 6 shows the variation of four kinds of ballistic limit velocities V_{bt} , V_{bt1} , V_{bt2} , and V_{50} with an increasing plate-thickness t for B_n and C_n plates, where V_{bt} is estimated from the analytical model and V_{bt2} from the modified one for impact velocity range far away from the ballistic limit velocity. All these ballistic limit velocities increase almost linearly with an increasing plate thickness and V_{50} provides the greatest ballistic limit velocity followed in order by V_{bt1} , V_{bt} , and V_{bt2} the smallest.

Figure 7 shows the comparison of ballistic limit velocities V_{bt} between two quasi-isotropic CFRP laminates with different stacking sequence (B_n and C_n). Since both are almost the same, the difference of the stacking sequence in quasi-isotropic laminates is found to little affect the ballistic limit velocity. In addition, the ballistic limit velocities of the orthotropic laminates A_2 and A_3 are confirmed to be almost the same as those of B_n and C_n for the identical plate-thickness. The ballistic limit velocities of aluminium A5052 plates (A_{lu}) and quasi-isotropic GFRP laminates (Gf_n) are also shown in Fig. 7 for comparison [8].

5. CONCLUSIONS

Perforation characteristics of the orthotropic and the quasi-isotropic carbon fiber composite target plates by a steel ball projectile have been investigated both experimentally and analytically. Two analytical models are introduced, namely, one is model A based solely on the conservation law of energy while the model B is based on the conservation laws of momentum and energy. By combining

these models with the impact test results, simple semi-empirical expressions for estimating a ballistic limit velocity and predicting a residual velocity are obtained.

Acknowledgements

The author wishes to thank Messrs. Y. Okayasu and H. Arai for their assistance in conducting the experimental work and data reduction.

REFERENCES

1. M. E. Backman and W. Goldsmith, The mechanics of penetration of projectiles into targets, *Int. J. Engng Sci.* **16**, 1–99 (1978).
2. G. G. Corbett, S. R. Reid and W. Johnson, Impact loading of plates and shells by free-flying projectiles, *Int. J. Impact Engng* **18** (2), 141–230 (1996).
3. S. Abrate, Impact of laminated composite materials, *Appl. Mech. Rev.* **44** (4), 155–190 (1991).
4. S. Abrate, Impact on laminated composites, *Appl. Mech. Rev.* **47** (11), 517–544 (1991).
5. S. Abrate, *Impact on Composite Structures*. Cambridge University Press (1998).
6. H. Kasano, Recent advances in high-velocity impact perforation of fiber composite laminates, *JSME International Journal, Series A* **42** (2), 147–157 (1999).
7. R. F. Recht and T. W. Ipson, Ballistic perforation dynamics, *J. Appl. Mech.* **30**, 384–390 (1963).
8. Unpublished.